Causes of SiH_4 dissociation in silane dc discharges

D. A. Doughty* and A. Gallagher†

Joint Institute for Laboratory Astrophysics, University of Colorado and National Insitute of Standards and Technology, Boulder, Colorado 80309-0440

(Received 4 June 1990)

Hydrogenated amorphous-silicon (*a*-Si:H) film growth on glass fibers strung between discharge electrodes is used to measure the distribution of film-producing radicals in a silane dc discharge. The measured distribution, as well as film deposition rates on the electrodes, show that typically $> 80\%$ of the depositing radicals are produced in the cathode sheath. Discharge models, confirmed by the spatial distribution of optical emission, rule out the possibility that this dissociation in the sheath is due to electron impact. Collisions of energetic ions and neutrals with silane are clearly implicated as the cause of this sheath dissociation. In contrast, due to much lower ion kinetic energies, almost all dissociation is due to electron collisions in the low-power rf discharges most commonly used for film production. In addition, the ratio of the number of Si atoms deposited on all surfaces to the total number of ions collected at the dc-discharge cathode is measured to be 30, demonstrating the dominance of neutral radical deposition in these discharges.

I. INTRODUCTION

Low-pressure glow-discharge decomposition of silane is the most common technique used to produce hydrogenated amorphous-silicon (*a*-Si:H) thin films.[1] Both rf and dc glow discharges can be used to produce *a*-Si:H films, but the rf system is the predominant configuration, in part because the substrate is not limited to being a conductor. In general, the films produced in a dc diode discharge (two parallel-plate electrodes) are of a poorer quality than those from a rf discharge. A dc configuration using three electrodes ("dc proximity") does produce high-quality films, probably because the energetic neutral and ion bombardment of the substrate is greatly reduced. The dc discharge has been important to understanding many fundamental aspects of a silane plasma. For example, ion chemistry in a dc silane glow discharge has been studied by Weakliem *et al.*,[2] Perrin *et al.*,[3] and by Chatham and Gallagher.[4] Robertson and Gallagher measured radicals at the cathode surface of a dc silane discharge,[5] and Drevillon *et al.*[6] studied the effects of ion bombardment on film density. Spectroscopic studies of neutral radicals have been done in silane dc discharges.[7,8]

We have applied our recently developed fiber-probe discharge diagnostic[9] to the dc silane discharge to measure the spatial distribution of film-producing radicals between the anode and the cathode. This measurement reveals a fundamental difference between the SiH_4 dissociation mechanism in dc versus rf discharges, and explains the large ratio of neutral versus ion deposition in dc discharges.

II. EXPERIMENT

The apparatus used to deposit *a*-Si:H films (see Fig. 1 of Ref. 9) consists of stainless-steel parallel-plate electrodes (7×12 cm^2) separated by 3.8 cm. The electrode assembly is placed in a close-fitting Pyrex tube, which is evacuated by a turbomolecular pump. The temperature of the electrodes is controlled by externally heating the entire discharge volume. Silane gas flows through the 20–250 °C discharge region at ~ 15 SCCM (where SCCM denotes cubic centimeter per minute at STP) while the density in this region is normally maintained at 5×10^{15} cm^3 (equivalent to 250 mT at 250 °C). A dc power supply delivers ~ 1 W which depletes $\sim 10\%$ of the silane under steady-state flowing conditions. For this electrode separation and silane density the cathode fall and negative glow regions are well developed; by visual inspection we observe the cathode fall to be ~ 2 cm long.

The spatial distribution of film growth is measured using 40-μm-diam glass fibers strung between the electrodes. This technique and apparatus is described in detail in Ref. 9. Briefly, as the discharge is run, film coats the fibers in proportion to the local density of depositing species times their deposition probability. (As discussed below, film growth on the electrodes greatly exceed ion current. Thus we assume that on the fibers as well film growth is proportional to the local density of depositing neutral radicals and independent of ions.) After depositing ~ 1 μm of film, the fibers are removed from the discharge and the film thickness on the fibers is measured. This is accomplished by scattering a He-Ne laser beam off a fiber and measuring interference fringes. The laser scans the length of the fiber and the interference oscillations are converted to film thickness $T(x)$ versus position on the fiber. Figure 1(a) shows $T(x)$ on a fiber coated in a 150 mT discharge at 20 °C, in which the discharge voltage was 600 V at a current of 1.8 mA.

In Sec. III this film-thickness data will be compared to the optical emission from the discharge. The spatial variation of 414 nm, SiH ($A\,^2\Delta \rightarrow X\,^2\Pi$), and 653-nm ($H_\alpha$) emission is measured by imaging the discharge region onto an optical multichannel analyzer through interference filters. Figure 1(c) shows the spatial distribution of

 ©1990 The American Physical Society

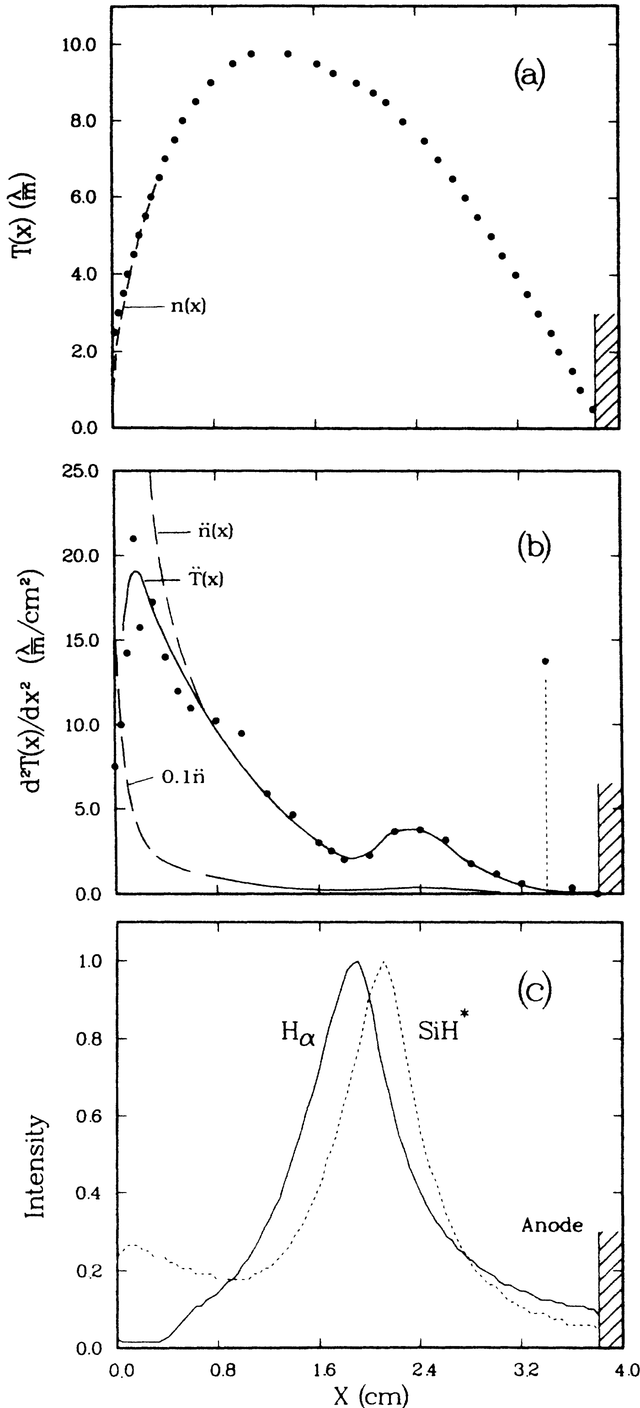

FIG. 1. (a) Measured *a*-Si:H film thickness vs distance from the cathode X on a 40-μm-diam glass fiber coated in a silane dc discharge. The film thickness T is in units of $\lambda/n_f \cong 0.2$ μm where λ is the laser wavelength used to scan the fiber and $n_f \cong 0.2$ μm, is the index of refraction of the *a*-Si:H film. Each dot represents the position of a fringe maximum or minimum as shown in Ref. 9. The dashed line near the cathode is a correction for changing incorporation. (b) The second derivative of the film thickness vs position (dots and solid line). The dashed line near the cathode results from the dashed-line correction in (a). (c) Normalized 414-nm (SiH^*) and 653-nm (H_α) light emission from the same discharge. The position of the anode is indicated by the shaded region.

414- and 653-nm light intensity from the discharge used to coat the fiber described above.

Also of interest to the following discussion is the ratio D_T/D_+ where D_T is the number of Si atoms deposited on all surfaces and D_+ is the total number of ions collected at the cathode. This measures how much film is derived from neutral radicals and how much from Si-bearing ions. To measure D_T/D_+ we enclose the electrodes with perforated glass plates (to maintain adequate gas flow between the electrodes) and run the discharge for a prescribed time. The electrode assembly is then disassembled and the film thickness on all surfaces is measured by scanning a He-Ne laser beam across the surfaces and recording the reflected intensity. The resulting interference fringes are converted to *a*-Si:H film thickness with a knowledge of the laser wavelength (633 nm) and the film index of refraction ($n_f = 3$ at 633 nm for a film deposited at 20 °C).[10] The film volume times the Si-atom number density ($\sim 5\times10^{22}$ atoms/cm^3) gives the total number of Si atoms deposited. We take D_+ to be the product of the discharge current and the time the discharge was operated. This is an approximation because: (i) the ion current at the cathode is slightly less than the total current due to secondary electrons; (ii) some ions may carry more than one Si atom and some carry none.

We measure $D_T/D_+ = 30$, with $\sim 68\%$ of D_T on the cathode, $\sim 14\%$ on the anode, and the remainder on the glass plates at the electrode edges. Uncertainties in the D_T/D_+ ratio and these percentages arise primarily from uncertainties in film index of refraction, which may be different for cathodic versus anodic and side-surface films, uncertainties in the fraction of the total cathode current carried by ions, and uncertainty in the average number of Si atoms per ion. These are 5–20% effects that partially cancel, and we conservatively estimate the overall uncertainty in D_T/D_+ to be $\pm 30\%$.

III. DISCUSSION

As an introduction to the following discussion we will first give a general description of the anatomy of a dc discharge.[11] A parallel-plate dc glow discharge can be conceptually divided into the cathode fall or "sheath" region, the negative glow region, and the positive column. At the gas density and electrode separation used for *a*-Si:H deposition without dust, the positive column does not form, so it will not be discussed here. The cathode fall region, adjacent to the cathode, is defined by a net positive space charge which produces a large electric field that decreases from a maximum at the cathode to ~ 0 at the cathode fall–negative glow boundary. Essentially the entire discharge voltage drop occurs across the cathode fall. Electrons released from the cathode are accelerated in this field, producing sufficient ionization to replace charges lost to the electrodes. The high field at the cathode also accelerates ions into the cathode surface, releasing the secondary electrons which are accelerated into the gas by the same field. The electric field strength self-adjusts so that, on average, the net ionization initiat-

ed by one secondary electron produces sufficient ions (typically ~ 10) to release one electron when they bombard the cathode. An electron avalanche occurs in the cathode fall since each ionization event produces an additional electron that can accelerate and further ionize the gas. This avalanche grows away from the cathode until the electric field becomes too small to accelerate new electrons to the ionization potential of the gas. This point marks the transition to the negative glow region, where the electric field is very small and more or less constant, and where the ion and electron densities are nearly equal. Highly directed high-energy electrons continue into the negative glow region, where they dissipate their energy in further excitations and ionizations. These characteristics, as well as typical electric fields, charge densities, and silane discharge parameters can be found in Ref. 4.

Electron impact dissociative excitation is expected to dominate light emission in silane discharges. As the electron avalanche grows away from the cathode so does this light intensity, until the cathode fall–negative glow boundary is reached. The avalanche is then halted but the high-energy electrons continuing into the negative glow cause the light intensity to gradually decrease toward the anode. We thus interpret the region of the intensity peaks in Fig. 1(c), $X \cong 2$ cm, as the cathode fall–negative glow boundary, and 2 cm as the "sheath" thickness inferred in Ref. 4. Due to the low electric field in the negative glow the electron density is considerably larger there, but these "bulk" electrons have very low energies and are incapable of dissociating silane or producing light. Near the cathode the discharge current is carried primarily by ions, while in the negative glow the electrons dominate due to their much larger drift velocity relative to ions. Since nearly all of the applied potential is dropped across the cathode fall, where the ion current dominates, most of the input power is given to the ions. A large fraction of this is dissipated by energetic impacts on the cathode.

As shown by our measurement of $D_T/D_+ \cong 30$, neutral radicals are the dominant film-producing species in this dc silane discharge. In the rf discharge we have shown that diffusing neutral radicals (SiH_3 and perhaps some nonreactive disilane radicals) are responsible for film growth.[9] This was also found to be true in the dc case: Robertson and Gallagher found the SiH_3 concentration at the cathode surface to be > 50 times any of the other monosilicon radicals,[5] while disilicon radicals were about 20% of SiH_3. This dominance of SiH_3 deposition is consistent with the known fast reactions of Si, SiH, and SiH_2 with SiH_4,[12–14] which keep their densities low. We will thus interpret the present data in terms of depositions by neutral radicals that are nonreactive in the gas.

We wish to interpret $T(x)$ in Fig. 1(a) to determine the source of depositing neutral radicals, as was done in Ref. 9. Neutral radicals are produced with a distributed source $S(x)$. If they diffuse to the electrodes without gas reactions, as expected for the dominant film-producing radicals, then for infinite-plane-parallel geometry with negligible loss to the fibers,

$$S(x) = -D d^2 n(x)/dx^2 , \tag{1}$$

where D is the diffusion coefficient.[9] Figure 1(b) contains a plot of d^2T/dx^2 derived from the data Fig. 1(a). In the rf discharge of Ref. 9, T is proportional to n, so that d^2T/dx^2 quantitatively maps $S(x)$. In this dc case, however, this proportionality breaks down. The problem is that the film growth rate and thus $T(x)$ is proportional to $s(x)n(x)$, where s is the Si incorporation probability per surface collision. In the rf silane discharge $s(x)$ is not expected to vary in different regions of the discharge, because the same neutral specie (SiH_3) dominates deposition everywhere and ions do not have a significant effect, and thus $T(x) \propto n(x)$.[9] But in dc discharges we expect $s(x)$ to be different in the cathode fall compared to the negative glow. One reason to expect this is an observed difference in the surface reaction probability β for film-producing radicals reacting at the cathode and anode of a silane dc discharge. This was measured for the same discharge conditions used for the data of Fig. 1(a) (Ref. 15) with the result $\beta_K = 0.59$ and $\beta_A = 0.33$, where the subscripts K and A refer to the cathode and anode. Here $\beta = s + \gamma$, where γ is the probability that the radicals react on the surface without incorporation (e.g., SiH_3 abstraction of a surface H atom to form SiH_4). The fact that β nearly doubles from the anode to the cathode suggests that s also increases substantially.

A second indication of changes in s comes from the fact that $-Ddn/dx$ at each surface should equal the radical flux to that surface, regardless of the value of β at the surface. The ratio of film thickness on the cathode versus anode was measured to be 5, but for the data in Fig. 1(a) $|dT(x)/dx| \equiv |\dot{T}(x)|$ at the cathode is only ~ 2.5 times as large as at the anode. Also, in Fig. 1(c) the $T(x)$ data extrapolate to zero at a distance α_K beyond the cathode and α_A beyond the anode. Since each α is proportional to $(2-\beta)/\beta$, α_K should actually be ~ 0.5 as long as α_A, whereas $\alpha_K \cong 2\alpha_A$ in Fig. 1(a). This α_K/α_A ratio as well as $|\dot{T}(0)/\dot{T}(3.8 \text{ cm})|$ in Fig. 1(a) can be made consistent with these requirements by assuming that $n(x)$ follows the dashed line at the left edge of Fig. 1(a) and the $T(x)$ data elsewhere. Since $s(x)n(x) \propto T(x)$, the ratio of the dashed line to the data at the left side of Fig. 1(a) corresponds to $s_A/s(x)$. This ratio is 0.3–0.5 at the cathode, consistent with expectations based on $\beta_K \cong 2\beta_A$ as noted in the previous paragraph. $\ddot{T}(x)$, and $\ddot{n}(x)$, from the dashed line and data points in Fig. 1(a) are shown in Fig. 1(b). Here the exact shape of the $\ddot{n}(x)$, which is proportional to the radical source, is somewhat uncertain near the cathode, but the fact that it is very sharply peaked at $x = 0$ is an inescapable conclusion.

Another, much smaller anomaly in the $T(x)$ data occurs at $x = 3.4$ cm, where $\dot{T}(x)$ undergoes an abrupt $\sim 15\%$ change. This is not evident in Fig. 1(a), but was reproducibly and clearly discerned in more detailed, expanded data sets at $T = 250$ and 20 °C. Thus, it is shown as an anomalous point at $x = 3.4$ cm in Fig. 1(b). We do not believe this point represents a source of film-producing radicals. Rather, we attribute it to a film-density decrease near the anode, since the Si deposition rate is actually proportional to film mass. We also observed that for $T = 20$ or 250 °C the film on the anode electrode etched much faster in NaOH than the cathode

film, implying that the anode film is more porous and less dense.

The mechanism by which film-producing radicals are initially produced in a silane glow discharge is generally assumed to be electron-impact dissociation of SiH_4. Furthermore, at the discharge powers and voltages used for film deposition, this dissociation is by electrons with energies above the 8-eV excitation threshold. To map the source of this electron-induced dissociation we have measured the optical emission from the discharge, as shown in Fig. 1(c). This optical emission arises from dissociative excitation by electron collision, which is also due to high-energy electrons. Thus it maps electron-collisional dissociation as well if: (i) the light is produced by electron collision with stable molecules (H_2, SiH_4, Si_2H_6) that are uniformly distributed, and (ii) the radiating state is short lived, so that the excited molecule does not diffuse a significant distance before emission occurs. H_α emission arises primarily from the dissociative excitation processes $e^- + H_2 \rightarrow e^- + H + H^*$ and $e^- + SiH_4 \rightarrow e^- + SiH_3 + H^*$, where H^* has a short (<200 ns) radiative lifetime.[16] (H_2 results from the overall process of converting silane to a-Si:H film and H_2.) Similarly, the band emission around 414 nm also arises from dissociative excitation:[17] $e^- + SiH_4 \rightarrow e^- + SiH^* + H_2 + H$ where SiH^* has a lifetime of 530 ns.[18]

The shape of the H_α light intensity in Fig. 1(c) is typical of that found in a dc glow discharge (see the discussion at the beginning of this section). The SiH^* intensity distribution is similar to the H_α curve in the negative-glow region, although it peaks slightly further from the cathode. This small shift is attributed to the different thresholds (10 eV for SiH^* and ~17 eV for H_α),[19,20] perhaps enhanced by differences in the behavior of the respective cross sections versus energy. Similar behavior and cause are reported for N_2 discharges in Ref. 21 (e.g., Fig. 11). The increase in 414-nm emission as the cathode is approached, however, is very different from a typical dc discharge and from the H_α emission. This will be discussed further below.

If electron-impact dissociation of SiH_4 is the production mechanism for the film-producing radicals then $d^2n(x)/dx^2$, shown in Fig. 1(b), should have a similar spatial character as the light curves in Fig. 1(c). The minor peak in Fig. 1(b) between $x=2$ and 3 cm does correlate with the peak of the light curves, so we attribute this peak to electron collisional dissociation of SiH_4. (The light curve is slightly closer to the cathode because the threshold for neutral dissociation [8 eV (Ref. 22)] is lower than the threshold for SiH^* production (10 eV).) As can be seen in Fig. 1(b), most of the depositing radicals are produced instead in the cathode sheath region ($x=0$ to 2 cm). Only ~10% of the area in Fig. 1(b) is attributable to the electron-impact dissociation contribution.

The most likely mechanism to account for the radical production is dissociation of SiH_4 by collisions with energetic ions and neutral atoms and molecules (energetic neutral atoms and molecules are created via charge exchange and fragmentation in ion-SiH_4 collisions). To see if ion energies are consistent with this, we note that from the high-field mobility estimated by Chatham and Gallagher[4] for silane ions in silane we estimate an average laboratory-frame ion energy at the cathode to be ~20 eV in the ~650 V dc discharge and ~3 eV in the rf case (150-V peak-to-peak rf voltage). This mobility results from assuming a collision cross section independent of energy, which is typical of a hard-sphere or charge-exchange cross section. These ion energies are consistent with the apparent absence of a dissociation source in the sheath region of the rf silane discharge, and its obvious presence in our dc discharge data. Fisher and Armentrout have measured the dissociation cross section Q_D, of $Ar^+ + SiH_4 \rightarrow$ products; they find that Q_D decreases with increasing energy at low ion energies (<5 eV), but then increasing dramatically for ion energies greater than 5 eV.[23] Silane dissociation due to SiH_n^+ collisions should be similar, so that ion-collisional dissociation should be very important in the dc sheath. It appears very probable that these energetic ion-SiH_4 collisions produce many H atoms, most of which have considerable kinetic energy (>0.2 eV). This is sufficient to overcome small reaction barriers, so that H abstraction occurs within a few H-SiH_4 collisions, before the H atoms have diffused as much as 1 mm. The SiH_3 so produced then causes the measured film deposition. The observed very sharp peak in $\ddot{n}(x)$ at the cathode is consistent with the expected rapid increase in ion energies near the cathode, combined with a ~5-eV threshold for these dissociations.

The 414-nm intensity in the vicinity of the cathode in Fig. 1(c) is almost certainly also due to energetic ion collisions, since the electron density is far too low in the sheath region to produce significant emission.[24,25] Furthermore, if electrons were responsible for this emission in the cathode fall region, then there would be H_α light as well. The absence of significant H_α light near the cathode indicates that the cross section for dissociative excitation of H_2 and SiH_4 to H^* by energetic ion collision is smaller than for the $SiH_4 \rightarrow SiH^*$ (414-nm) process. Part of the reason for this may be the smaller enthalpy difference for the 414-nm process (9.2 eV) compared to the H_α process (14.3 eV from H_2).

From known electron-impact dissociation (Q_T) and ionization (Q_+) cross sections[22,26] of SiH_4, combined with silane radical and ion chemistry, we can estimate D_T/D_+ that would result from only electron collisions. The cross

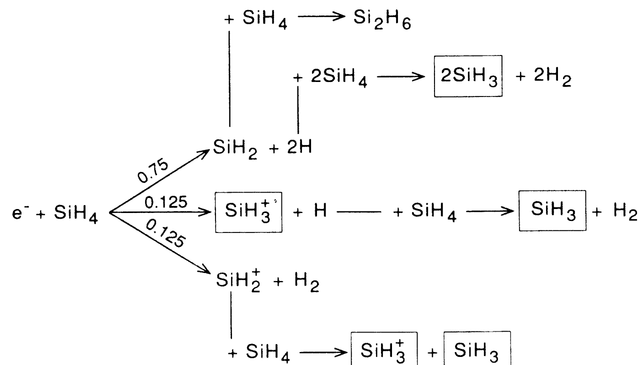

FIG. 2. Illustration of how electron-induced dissociation of SiH_4 results in stable products after gas phase reactions. The boxed species are stable ion and neutral radicals.

sections peak at ~60 eV electron energy, where $Q_+ = 6$ Å^2 and $Q_T = 12$ Å^2, while the dissociation threshold is ~8 eV and the ionization threshold is ~11 eV. Thus, a 60-eV electron will have an equal probability of producing dissociation to an ion or only neutral radicals, but lower energies favor the lower threshold process. Kushner has applied his electron Monte Carlo code[27] to our dc discharge conditions, and obtained a ratio of ~3 for the volume-averaged neutral dissociation versus ionization rate. The principal neutral dissociation pathway appears to be $SiH_2 + 2H$,[28] whereas ion dissociation primarily results in $SiH_2^+ + H_2$ and $SiH_3^+ + H$ with roughly equal probabilities.[26] Using the simplified scheme in Fig. 2 for subsequent gas-phase reactions then leads to 1.75 SiH_3 and 0.25 Si-bearing ions reaching the surface for each electron-collisional dissociation, with a total of 3.5 SiH_4 consumed. Assuming two SiH_3 surface reactions are required to produce one film Si atom, this yields $D_T/D_+ = 4.5$. Thus, if only electron-collisional dissociation occurred, we would expect ion deposition to be ~22% of the total, compared to the ~3% measured.

Since energetic ion collisions produce ~10 times as many net depositions as electron collisions [Fig. 1(b)], their products dominate the deposition chemistry and D_T/D_+. Apparently each ion produces ~30 deposited Si atoms by dissociative collision cascade while traversing the gas, since $D_T/D_+ \cong 30$. As already noted, each ion-SiH_4 collision doubtless produces H as well as SiH_n radicals, and collision cascades of energetic neutrals can also contribute.

IV. CONCLUSION

We have used 40-μm-diam glass fiber probes to measure the distributed source of depositing radicals in the dc silane discharge. From this measurement we find that major SiH_4 dissociation is occurring in the cathode sheath region. Optical emission from the discharge maps primarily the dissociation due to electron impact; a comparison of this optical emission and the measured source function reveals that electrons are not causing the dissociation in the sheath. We believe the collisions of energetic ions and neutral atoms and molecules with silane is the primary cause of this enhanced source in the sheath. This explains why we observe significant 414-nm emission in the vicinity of the cathode, why the ratio of film on the cathode to that on the anode is so large, and why neutral radicals contribute 30 times as much Si to the *a*-Si:H film as do the ions.

ACKNOWLEDGMENTS

This work is supported by the Solar Energy Research Institute. We gratefully acknowledge Mark Kushner for performing Monte Carlo calculations used in this work, and appreciate many valuable discussions with J. R. Doyle.

---

*Present address: General Electric Co., P.O. Box 8, Bldg. K1-4C28, Schenectady, NY 12301.

†Also at Quantum Physics Division, National Institute of Standards and Technology, Boulder, CO 80309.

[1]W. Luft and S. Tsuo, Appl. Phys. Commun. **8**, 1 (1988).

[2]H. A. Weakliem, R. D. Estes, and P. A. Longeway, J. Vac. Sci. Technol. A **5**, 29 (1987).

[3]J. Perrin, A. Lloret, G. deRosny, and J. P. M. Schmitt, Int. J. Mass Spectrom. Ion Proc. **57**, 249 (1984).

[4]H. Chatham and A. Gallagher, J. Appl. Phys. **58**, 159 (1985).

[5]R. Robertson and A. Gallagher, J. Appl. Phys. **59**, 3402 (1986).

[6]B. Drevillon, J. Perrin, J. M. Siefert, J. Huc, A. Lloret, G. deRosny, and J. P. M. Schmitt, Appl. Phys. Lett. **42**, 801 (1983).

[7]J. M. Jasinski, E. A. Whittaker, G. C. Bjorklund, R. W. Dreyfus, R. D. Estes, and R. E. Walkup, Appl. Phys. Lett. **44**, 1155 (1984).

[8]C. Yamada and E. Hirota, Phys. Rev. Lett. **56**, 923 (1986).

[9]D. A. Doughty and A. Gallagher, J. Appl. Phys. **67**, 139 (1990).

[10]G. Myburg and R. Swanepoel, Jpn. J. Appl. Phys. **27**, 899 (1988).

[11]J. H. Ingold, in *Gaseous Electronics,* edited by M. N. Hirsh and H. J. Oskam (Academic, New York, 1978), Vol. 2.

[12]M. E. Coltrin, R. J. Kee, and J. A. Miller, J. Electrochem. Soc. **131**, 425 (1984).

[13]J. P. M. Schmitt, P. Gressier, M. Krishnan, G. deRosny, and J. Perrin, Chem. Phys. **84**, 281 (1984).

[14]J. M. Jasinski and J. O. Chu, J. Chem. Phys. **88**, 1678 (1988).

[15]D. A. Doughty, J. R. Doyle, G. H. Lin, and A. Gallagher, J. Appl. Phys. (to be published).

[16]W. L. Wiese, M. W. Smith, and B. M. Glennon, *Atomic Transition Probabilities* (U.S. GPO, Washington, D.C., 1966), p. 2.

[17]F. J. Kampas and R. W. Griffith, J. Appl. Phys. **52**, 1285 (1981).

[18]J. P. M. Schmitt, P. Gressier, M. Krishnan, G. deRosny, and J. Perrin, Chem. Phys. **84**, 281 (1984).

[19]J. Perrin and J. F. M. Aarts, Chem. Phys. **80**, 351 (1983).

[20]G. R. Möhlmann, F. J. deHeer, and J. Los, Chem. Phys. **25**, 103 (1977).

[21]S. Radovanov, B. Tomcik, Z. L. Petrović, and B. M. Jelenković, J. Appl. Phys. **67**, 97 (1990).

[22]J. Perrin, J. P. M. Schmitt, G. deRosny, B. Drevillon, J. Huc, and A. Lloret, Chem. Phys. **73**, 383 (1982).

[23]E. R. Fisher and P. B. Armentrout (private communication).

[24]M. J. Kushner, J. Appl. Phys. **54**, 4958 (1983).

[25]T. J. Moratz, J. Appl. Phys. **63**, 2558 (1988).

[26]H. Chatham, D. Hils, R. Robertson, and A. Gallagher, J. Chem. Phys. **81**, 1770 (1984).

[27]M. J. Kushner, J. Appl. Phys. **63**, 2532 (1988).

[28]J. Doyle, D. Doughty, and A. Gallagher, J. Appl. Phys. (to be published).